ISSN 1948-0210 (online)

World Journal of *Stem Cells*

World J Stem Cells 2023 July 26; 15(7): 654-780

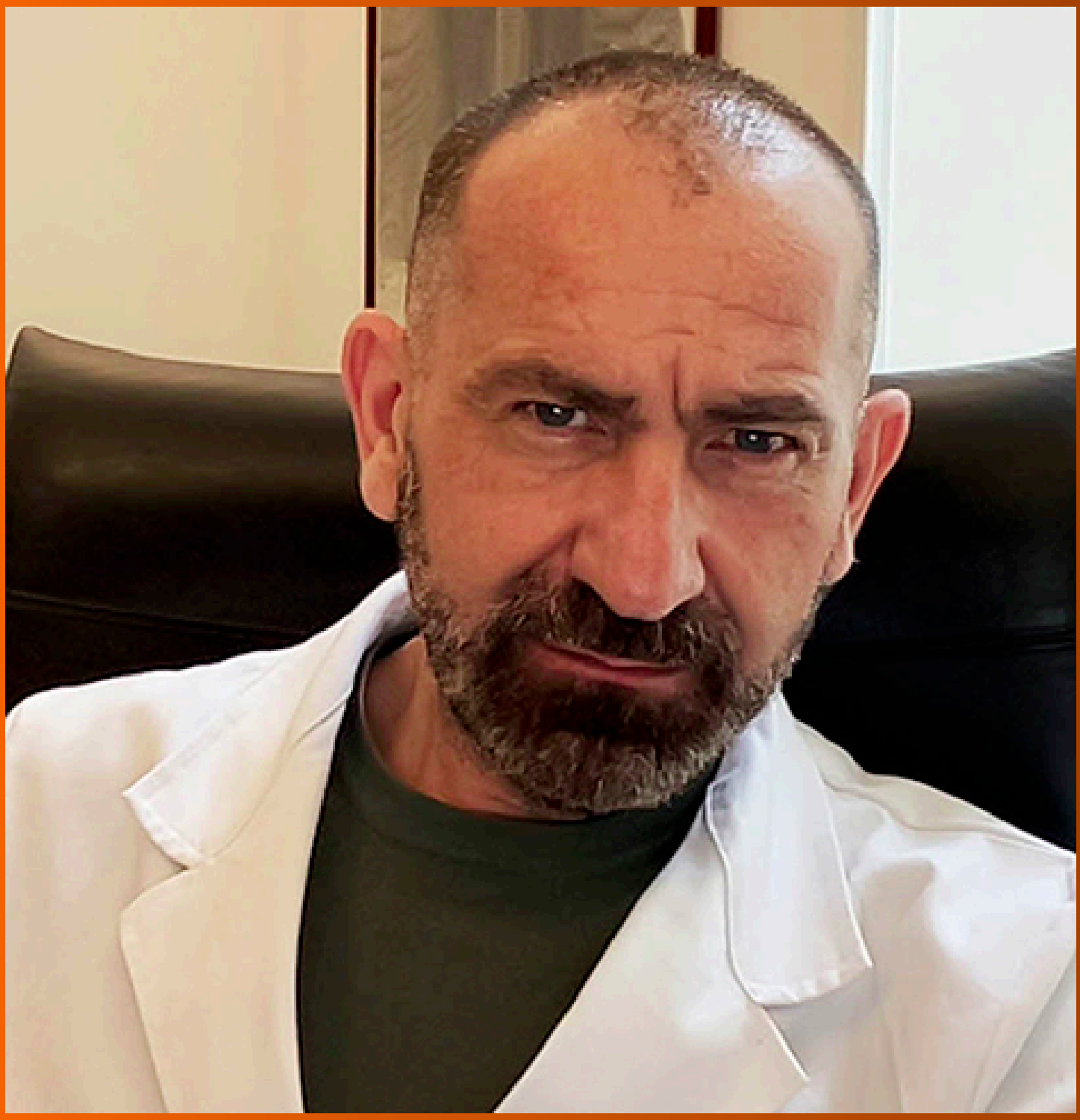

Published by Baishideng Publishing Group Inc

WJSC

World Journal of Stem Cells

Contents

Monthly Volume 15 Number 7 July 26, 2023

OPINION REVIEW

REVIEW

MINIREVIEWS

ORIGINAL ARTICLE

Basic Study

World Journal of Stem Cells

Monthly Volume 15 Number 7 July 26, 2023

Contents

ABOUT COVER

Editorial Board Member of *World Journal of Stem Cells*, Giovanni Di Bernardo, BSc, PhD, Associate Professor, Department of Experimental Medicine, Biotechnology and Molecular Biology Section, University of Campania Luigi Vanvitelli, Naples 80138, Italy. gianni.dibernardo@unicampania.it

AIMS AND SCOPE

The primary aim of *World Journal of Stem Cells* (*WJSC*, *World J Stem Cells*) is to provide scholars and readers from various fields of stem cells with a platform to publish high-quality basic and clinical research articles and communicate their research findings online. *WJSC* publishes articles reporting research results obtained in the field of stem cell biology and regenerative medicine, related to the wide range of stem cells including embryonic stem cells, germline stem cells, tissue-specific stem cells, adult stem cells, mesenchymal stromal cells, induced pluripotent stem cells, embryonal carcinoma stem cells, hemangioblasts, lymphoid progenitor cells, *etc*.

INDEXING/ABSTRACTING

The *WJSC* is now abstracted and indexed in Science Citation Index Expanded (SCIE, also known as SciSearch®), Journal Citation Reports/Science Edition, PubMed, PubMed Central, Scopus, Biological Abstracts, BIOSIS Previews, Reference Citation Analysis, China National Knowledge Infrastructure, China Science and Technology Journal Database, and Superstar Journals Database. The 2023 Edition of Journal Citation Reports® cites the 2022 impact factor (IF) for *WJSC* as 4.1; IF without journal self cites: 3.9; 5-year IF: 4.5; Journal Citation Indicator: 0.53; Ranking: 15 among 29 journals in cell and tissue engineering; Quartile category: Q3; Ranking: 99 among 191 journals in cell biology; and Quartile category: Q3. The *WJSC*'s CiteScore for 2022 is 8.0 and Scopus CiteScore rank 2022: Histology is 9/57; Genetics is 68/325; Genetics (clinical) is 19/90; Molecular Biology is 119/380; Cell Biology is 95/274.

RESPONSIBLE EDITORS FOR THIS ISSUE

NAME OF JOURNAL
World Journal of Stem Cells

ISSN
ISSN 1948-0210 (online)

LAUNCH DATE
December 31, 2009

FREQUENCY
Monthly

EDITORS-IN-CHIEF
Shengwen Calvin Li, Carlo Ventura

EDITORIAL BOARD MEMBERS
https://www.wjgnet.com/1948-0210/editorialboard.htm

PUBLICATION DATE
July 26, 2023

INSTRUCTIONS TO AUTHORS
https://www.wjgnet.com/bpg/gerinfo/204

GUIDELINES FOR ETHICS DOCUMENTS
https://www.wjgnet.com/bpg/GerInfo/287

GUIDELINES FOR NON-NATIVE SPEAKERS OF ENGLISH
https://www.wjgnet.com/bpg/gerinfo/240

PUBLICATION ETHICS
https://www.wjgnet.com/bpg/GerInfo/288

PUBLICATION MISCONDUCT
https://www.wjgnet.com/bpg/gerinfo/208

ARTICLE PROCESSING CHARGE
https://www.wjgnet.com/bpg/gerinfo/242

STEPS FOR SUBMITTING MANUSCRIPTS
https://www.wjgnet.com/bpg/GerInfo/239

ONLINE SUBMISSION
https://www.f6publishing.com

World Journal of Stem Cells

Submit a Manuscript: https://www.f6publishing.com

World J Stem Cells 2023 July 26; 15(7): 701-712

DOI: 10.4252/wjsc.v15.i7.701

ISSN 1948-0210 (online)

ORIGINAL ARTICLE

Basic Study

Commitment of human mesenchymal stromal cells to skeletal lineages is independent of their morphogenetic capacity

Jessica Cristina Marín-Llera, Damián García-García, Estefania Garay-Pacheco, Victor Adrian Cortes-Morales, Juan Jose Montesinos-Montesinos, Jesus Chimal-Monroy

Specialty type: Cell and tissue engineering

Provenance and peer review: Invited article; Externally peer reviewed.

Peer-review model: Single blind

Peer-review report's scientific quality classification
Grade A (Excellent): 0
Grade B (Very good): B, B
Grade C (Good): C
Grade D (Fair): 0
Grade E (Poor): 0

P-Reviewer: Shamseldeen AM, Egypt; Yang YZ, China

Received: December 29, 2022
Peer-review started: December 29, 2022
First decision: April 27, 2023
Revised: May 18, 2023
Accepted: June 25, 2023
Article in press: June 25, 2023
Published online: July 26, 2023

Jessica Cristina Marín-Llera, Damián García-García, Estefania Garay-Pacheco, Medicina Genómica y Toxicología Ambiental, Instituto de Investigaciones Biomédicas, Universidad Nacional Autónoma de México, Coyoacan 04510, Mexico

Victor Adrian Cortes-Morales, Juan Jose Montesinos-Montesinos, Laboratorio de Células Troncales Mesenquimales, Unidad de Investigación Médica en Enfermedades Oncológicas, Hospital de Oncología Centro Medico Nacional Siglo XXI, Instituto Mexicano del Seguro Social, Mexico City 06720, Mexico

Jesus Chimal-Monroy, Departamento de Medicina Genómica y Toxicología Ambiental, Instituto de Investigaciones Biomédicas, Universidad Nacional Autónoma de México, Coyoacan 04510, Mexico

Corresponding author: Jesus Chimal-Monroy, PhD, Research Scientist, Senior Researcher, Departamento de Medicina Genómica y Toxicología Ambiental, Instituto de Investigaciones Biomédicas, Universidad Nacional Autónoma de México, Ciudad Universitaria, Apartado Postal 70228, Coyoacan 04510, Mexico. jchimal@unam.mx

Abstract

BACKGROUND

Mesenchymal stromal cells (MSCs) are multipotent cell populations obtained from fetal and adult tissues. They share some characteristics with limb bud mesodermal cells such as differentiation potential into osteogenic, chondrogenic, and tenogenic lineages and an embryonic mesodermal origin. Although MSCs differentiate into skeletal-related lineages *in vitro*, they have not been shown to self-organize into complex skeletal structures or connective tissues, as in the limb. In this work, we demonstrate that the expression of molecular markers to commit MSCs to skeletal lineages is not sufficient to generate skeletal elements *in vivo*.

AIM

To evaluate the potential of MSCs to differentiate into skeletal lineages and generate complex skeletal structures using the recombinant limb (RL) system.

METHODS

We used the experimental system of RLs from dissociated-reaggregated human placenta (PL) and umbilical cord blood (UCB) MSCs. After being harvested and reaggregated in a pellet, cultured cells were introduced into an ectodermal cover

obtained from an early chicken limb bud. Next, this filled ectoderm was grafted into the back of a donor chick embryo. Under these conditions, the cells received and responded to the ectoderm's embryonic signals in a spatiotemporal manner to differentiate and pattern into skeletal elements. Their response to differentiation and morphogenetic signals was evaluated by quantitative poly-merase chain reaction, histology, immunofluorescence, scanning electron microscopy, and *in situ* hybridization.

RESULTS

We found that human PL-MSCs and UCB-MSCs constituting the RLs expressed chondrogenic, osteogenic, and tenogenic molecular markers while differentially committing into limb lineages but could not generate complex structures *in vivo*. MSCs-RL from PL or UCB were committed early to chondrogenic lineage. Nevertheless, the UCB-RL osteogenic commitment was favored, although preferentially to a tenogenic cell fate. These findings suggest that the commitment of MSCs to differentiate into skeletal lineages differs according to the source and is independent of their capacity to generate skeletal elements or connective tissue *in vivo*. Our results suggest that the failure to form skeletal structures may be due to the intrinsic characteristics of MSCs. Thus, it is necessary to thoroughly evaluate the biological aspects of MSCs and how they respond to morphogenetic signals in an *in vivo* context.

CONCLUSION

PL-MSCs and UCB-MSCs express molecular markers of differentiation into skeletal lineages, but they are not sufficient to generate complex skeletal structures *in vivo*.

Key Words: Human mesenchymal stromal cells; Recombinant limbs; Mesenchymal stromal cell morphogene-sis; Mesenchymal stromal cell *in vivo* differentiation; Skeletal tissues

Core Tip: Human mesenchymal stromal cells (MSCs) from umbilical cord blood or placenta can differentiate into osteogenic and chondrogenic lineages in culture systems and have been used in regenerative medicine. Here, we used the recombinant limb (RL) model to provide evidence that MSCs do not have the ability to generate skeletal structures *in vivo*. MSCs received and responded to the ectoderm's embryonic spatiotemporal signals in this RL system. However, the expression of differentiation markers of skeletal lineages was not sufficient to generate skeletal structures *in vivo*.

Citation: Marín-Llera JC, García-García D, Garay-Pacheco E, Adrian Cortes-Morales V, Montesinos-Montesinos JJ, Chimal-Monroy J. Commitment of human mesenchymal stromal cells to skeletal lineages is independent of their morphogenetic capacity. *World J Stem Cells* 2023; 15(7): 701-712

URL: https://www.wjgnet.com/1948-0210/full/v15/i7/701.htm

DOI: https://dx.doi.org/10.4252/wjsc.v15.i7.701

INTRODUCTION

The limbs have an intricate anatomy that results from highly coordinated morphogenesis and cellular differentiation processes, which establish the correct position and shape of muscles, bones, cartilage, tendons, skin, and nerves[1]. During embryonic development, limb bud mesodermal cells (LBMCs) form a bud covered by a layer of ectodermal cells. The morphogenesis and differentiation of limb tissues are controlled by the response to signals that emanate from three signaling centers: The apical ecto-dermal ridge (AER), which controls the proximodistal axis; the zone of polarizing activity, which directs the anteroposterior axis; and the ventral and dorsal LB ectoderms, which control the dorsal-ventral axis[1,2]. Fibroblast growth factor 8 (FGF8) and Wnt family member 3a signals emanate from the AER and maintain the MCs in an undifferentiated and proliferative state. Once cells stop receiving AER signals, they begin the differentiation process toward the chondrogenic and tenogenic lineages, followed by endochondral ossification to form the skeletal elements[1,2]. As development progresses, the coordination between signals is essential for patterning and differentiation to fully develop the skeletal elements of a functional limb[1,2].

SRY-box transcription factor 9 (SOX9) is the earliest molecular marker of chondrogenic commitment[3]. Besides, SOX9 induces the expression of extracellular matrix proteins such as collagen type 2 (Col2α) and aggrecan (ACAN)[4]. On the other hand, growth differentiation factor 5 (GDF5) promotes cell condensa-tion and cell adhesion during the initial stages of chondrogenesis[5,6]. By contrast, hypoxia-inducible factor alpha (HIF-1α) is critical in maintaining the chondrogenic environment[7]. Once cartilage anlagen is formed, ossification begins by expressing Runt-related transcription factor 2 (RUNX2)[8-10]. At the same time, the dorsal and ventral margins of early embryonic LB initiate tendon specification by express-ing the earliest known marker of tenocyte progenitors, scleraxis (SCX)[11,12]. SCX induces the transcription of major structural collagens and the glycoprotein tenomodulin[13]. Mohawk (MKX) is involved in tendon maturation by

maintaining SCX expression, which restricts cells to the tenogenic lineage[13,14].

Regenerative medicine has emerged as an alternative treatment for degenerative diseases or an adjuvant therapy[15,16]. To this end, the potential use of mesenchymal stromal cells (MSCs) has garnered great interest. Because MSCs share characteristics with LBMCs and have the potential to differentiate into osteogenic or chondrogenic lineages[17-21], in this work, we used the recombinant limb (RL) model to evaluate the capacity of human MSCs to form complex skeletal structures[22]. The RL model recapitulates the differentiation, morphogenesis, and patterning programs that occur during normal limb development[23-25]. RLs consist of an ectodermal cover obtained from an early chicken LB (CK-LB) filled with dissociated-reaggregated cells grafted into the back of a donor chick embryo. Because of the high capacity of human MSCs from umbilical cord blood (UCB-MSCs) or placenta (PL-MSCs) to differentiate into osteogenic and chondrogenic lineages, we evaluated their ability to generate skeletal structures *in vivo*. Our results demonstrate that although MSCs receive and respond to the ectoderm's embryonic spatiotemporal signals, they do not generate complex skeletal structures, possibly due to the intrinsic characteristics of MSCs.

MATERIALS AND METHODS

Isolation and culture of MSCs

MSCs were collected from Villa Coapa Hospital, Mexican Social Security Institute (IMSS; Mexico City, Mexico) according to their ethical guidelines, including informed consent. MSCs derived from bone marrow (BM; n = 3) were used to validate the specificity of all primers used in this study. BM cells were obtained from hematologically normal BM transplantation child donors at the Bernardo Sepulveda Hospital (National Medical Center, IMSS). A cell population enriched for MSCs was isolated according to Montesinos *et al*[25] using a negative selection procedure [RosetteSep™ system; STEMCELL Technologies Inc. (STI), Vancouver, Canada] and a Ficoll gradient. The cells were resuspended in low-glucose Dulbecco's modified Eagle medium (Lg-DMEM; Gibco BRL, Rockville, MD, United States) supplemented with 10% fetal bovine serum (FBS) and seeded at a density of 0.2 × 10^6 cells/cm^2 into T25 cell culture flasks (Corning Inc., Costar, New York, NY, United States). After 4 d, the nonadherent cells were removed by pipetting, and fresh medium was added. Every 5 d, a medium change was performed. When the cultures reached 80% confluence, they were trypsinized (0.05% trypsin, 0.53 mmol/L EDTA; Gibco BRL, New York, NY, United States) and subcultured at a density of 0.01 × 10^6 cells/cm^2 into T75 flasks (Corning). In the second passage, cells were harvested and analyzed.

UCB-MSC and PL-MSC samples were obtained from two volunteer donors from normal full-term deliveries according to the institutional guidelines of Troncoso Hospital, IMSS, as previously described by Montesinos *et al*[25]. UCB-derived MSCs were obtained using a negative selection procedure (RosetteSep™ system; STI), as described for BM. Cells were resuspended in Lg-DMEM (Gibco) supplemented with 10% FBS (STI) and seeded at a density of 0.2 × 10^6 cells/cm^2 in T25 culture flasks (corning), and subsequent cultures were manipulated as described for BM. PL-derived MSCs were obtained using an enzymatic digestion procedure. The internal area (about 2 cm^3) of the central PL lobules was washed with phosphate-buffered saline (PBS) and dissected into small pieces with sterilized scissors and forceps. The chopped tissues were digested with trypsin-EDTA (Gibco) at 37 °C for 10 min. A single-cell suspension was collected by flushing the tissue parts through a 100-μm nylon filter (Falcon; Becton, Dickinson and Company, San Jose, CA, United States) with Lg-DMEM containing 10% FBS. The cell suspension was centrifuged for 10 min at 400 g to collect the cell pellet. Then, the cells were resu-spended in Lg-DMEM supplemented with 10% FBS. The total number of nucleated and viable cells was determined, seeded, and manipulated as described for BM. After the third passage, the cells were analyzed and cryopreserved. For all experiments, MSCs were used in passages 4-5.

RLs

RLs were established according to the protocol by Marín-Llera *et al*[24]. PL-MSCs, UCB-MSCs, or 22 Hamburger-Hamilton (HH) CK-LBMCs were collected to stuff 22 HH CK limb ectoderms, according to Hamburger and Hamilton [26]. After obtaining PL-MSCs, UCB-MSCs, or CK-LBMCs, they were centrifuged at 3000 rpm and incubated at 37 °C between 1.5 h and 2 h to form a compact pellet. Separately, to obtain ectoderms, LBs from about 10 of the 22 HH embryos were dissected in PBS, transferred to a tube, and digested in 0.5% trypsin in PBS for 30 min at 37 °C. Then, the LBs were transferred to PBS supplemented with 10% FBS, and the ectoderm was peeled off. Next, the pellet of PL-MSCs, UCB-MSCs, or CK-LBMCs was detached from the bottom of the tube and transferred to a small petri dish containing the ectoderms. Later, a pellet fragment was stuffed into each ectoderm. Ectoderms were individually transferred into a previously windowed 22 HH chick embryo, positioned between somites 15-20, and fixed with palladium wires over a previously scratched wound. Manipulated embryos were incubated for 24 h, 48 h, or 72 h at 37.5 °C until their collection and processing. The leftover pellet from three sources was independently frozen to evaluate its basal expression compared to RLs by quantitative polymerase chain reaction (qPCR). All RL experiments were performed in triplicate.

qPCR

RNA from RLs was extracted with NucleoSpin RNA (Cat. No. 740955; Macherey-Nagel, Düren, Ger-many) according to the manufacturer's instructions. Retrotranscription of total RNA was achieved using the RevertAid RT Kit (Cat. K1691; Thermo Fisher Scientific, Waltham, MA, United States). Gene expression levels were quantified using SYBR green (Cat. No. 4309155; Thermo Fisher Scientific), normalizing to the transcript level of ribosomal protein L13. The expression level was evaluated relative to a calibrator according to the $2^{-\Delta\Delta Ct}$ equation. Each plotted value represents the mean ± SD of at least three independent experiments. For each independent qPCR replicate, RNA was obtained from 25 to 30 RL pools for each condition. In addition, leftover pellets of MSCs were collected and processed for RNA extraction. The student's t-test

was performed to compare the expression levels between pellets and RLs and to determine the statistical significance among RL sources. Statistical significance was set at $P < 0.05$. To analyze the specificity of the amplification, a melting curve was achieved for each primer. The specificity of all primers was validated with human MSCs-BM before amplification in the RL. The primer sequences used in this study are included in Supplementary Table 1.

Alcian blue and hematoxylin staining

For Alcian blue staining of RLs, samples were fixed in 5% trichloroacetic acid (Cat. No. A-5268; Sigma-Aldrich, St. Louis, MO, United States) for 24 h and stained with 1% Alcian blue in ethanol-hydrogen chloride for 24 h. Then, the RLs were transferred to 100% ethanol for 24 h and cleared with methyl salicylate (Cat. No. M-2047; Sigma-Aldrich) until the skeleton was observed. RL images were acquired with the AxioZoom v16 microscope (Carl Zeiss, Oberkochen, Germany) using ZEN lite software (Carl Zeiss). After image acquisition, Alcian blue-stained RLs were dehydrated in ethanol and xylol before embedding in paraffin. Ten-micrometer sections were obtained with a microtome (RM2125 RTS; Leica, Wetzlar, Germany). For hematoxylin and eosin (H&E) staining, samples were rehydrated with an ascending gradient of xylol-ethanol, followed by incubation with H&E dyes. Next, slides were dehydrated with ethanol-xylol and mounted with DPX medium (Cat. 44581; Sigma-Aldrich). Images were acquired with the Olympus BX51-WI microscope equipped with a fluorescence and gyratory disc unit (Tokyo, Japan) using Stereo Investigator 9 software (MicroBrightField Inc., Colchester, VT, United States).

Detection of cell death with LysoTracker staining

RLs were incubated in 1 μM LysoTracker Red DND-99 (Cat. L7528; Molecular Probes, Eugene, OR, United States) at 37 °C for 15 min. Then, the samples were rinsed with PBS and fixed in 4% paraformaldehyde overnight at 4 °C. Next, the RLs were dehydrated in an increasing methanol-PBS-Tween series and cleared with 2:1 benzylic alcohol-benzyl benzoate solution for 1 h (following the 1999 recommendations by Parish). Images were acquired with an Olympus BX51-WI microscope equipped with a fluorescence and gyratory disc unit using Stereo Investigator 9 software (MicroBrightField).

Scanning electron microscopy

RLs were washed twice with PBS and fixed in 2.5% glutaraldehyde in 0.1 M sodium cacodylate buffer (pH = 7.2) for 2 h. The fixation solution was washed three times with 0.1 M sodium cacodylate at 4 °C. For postfixation, samples were immersed in 1% osmium tetroxide in cacodylate solution for 2 h before dehydration in graded concentrations of ethanol. The samples were placed in microporous capsules submerged in pure ethanol and placed in the Critical Point drying equipment (SPI) for desiccation. Ethanol was replaced with liquid carbon dioxide until its critical constants (31.3 °C and 1072 PSI) were met. After drying, the sample was mounted on an aluminum specimen holder with a silver-based adhesive. The coating was performed by ionizing the sample with a layer of gold in a low vacuum ionizer. Images were acquired using the DSM-950 Carl Zeiss microscope.

In situ hybridization

RNA antisense probes were labeled with UTP-digoxigenin (Cat. No. 11209256910; Roche Applied Science, Indianapolis, IN, United States) and used for whole-mount *in situ* hybridization as previously described[6]. Samples were treated with 15 μg/mL proteinase K for 20 min at 21 °C, and the hybridization temperature was 68 °C. The *Fgf8* signal was visualized with BM Purple substrate for alkaline phosphatase (Roche). Images were acquired with the AxioZoom v16 microscope (Carl Zeiss).

RESULTS

RLs serve as a model to evaluate the morphogenesis and differentiation processes of human MSCs

We used RLs as an experimental model to evaluate the capacity of PL-MSCs and UCB-MSCs to differentiate into limb tissues and to determine their capacity to generate well-organized tissues in an *in vivo* context. In the first instance, we evaluated the competence of human MSCs to respond to embryonic signals present in the limb ectoderm (Figure 1). The results showed that 24 h postimplantation (hpi), the PL-MSCs and UCB-MSCs were successfully integrated and formed RLs, with an efficiency of 62.95% and 76.87%, respectively (Figure 1A). Next, we measured the expression and distribution of major histocompatibility complex 1 (HLA1) to determine whether the RLs were exclusively formed by MSCs. We observed that both MSCs-RLs expressed significantly higher levels of HLA1 compared with their own pellet before transplantation. In addition, the cells in the center of the RLs were HLA1$^+$ (Figure 1B). These results demonstrated the successful establishment of RLs composed of human MSCs for the evaluation of MSC behavior *in vivo*.

Morphology of MSCs changes as RL develops

To assess the capacity of human MSCs to form well-organized tissues, the phenotype of MSC-RLs and their cell organization were evaluated at 24 hpi, 48 hpi, and 72 hpi and compared with RLs formed with CK-LBMCs as a reference of the morphogenetic behavior under RL conditions. In contrast to CK-RL, no evidence of central skeletal elements was observed in RLs from either MSC source (Figure 2). Histolo-gical analyses revealed that the ectodermal cover in all RL conditions was maintained as a monostrati-fied epithelium, while cellular condensation in the center of the MSCs-RL was observed at all time points (Figure 2). Interestingly, the morphology of cell condensations in MSCs-RLs from both sources changed as the development of the RLs progressed, but UCB-RLs showed more evident progressive elongation of a

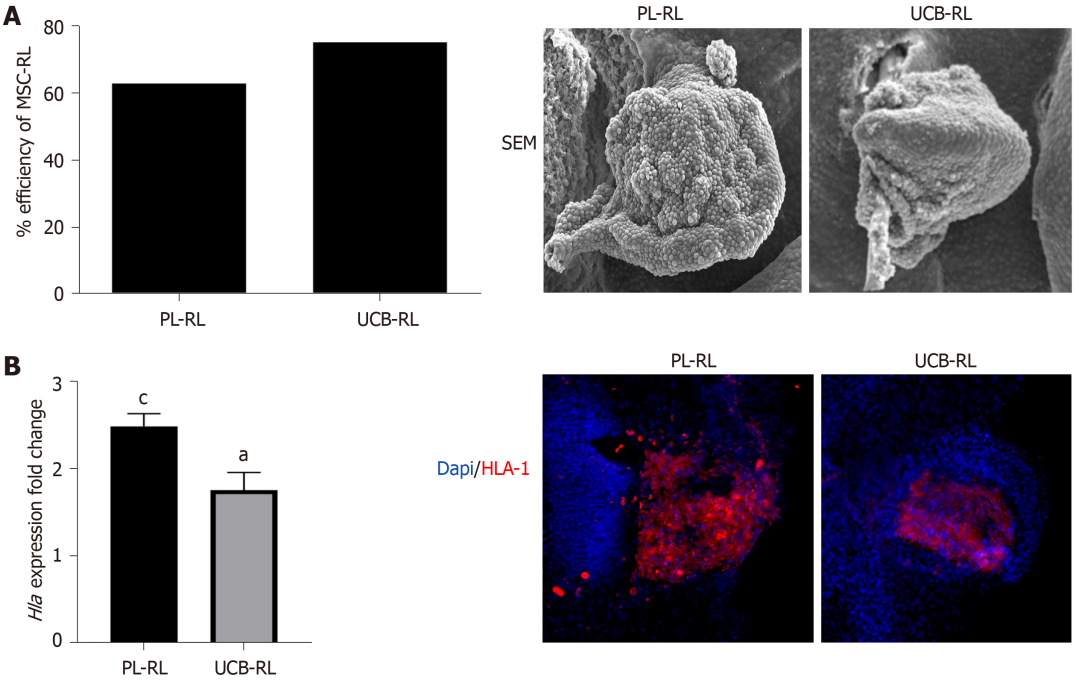

DOI: 10.4252/wjsc.v15.i7.701

Figure 1 Validation of the recombinant limb system using human mesenchymal stromal cells. A: Implantation efficiency of umbilical cord blood (UCB)-recombinant limb (RLs) and placenta (PL)-RLs in chicken embryos after 24 h. Scanning electron microscopy of PL-RLs (n = 3) and UCB-RLs (n = 2) at 24 h postimplantation (hpi). The embryonic ectoderm and apical ectodermal ridge were conserved in RLs from both sources; B: Levels of human leukocyte antigen (*Hla*) detected by quantitative polymerase chain reaction at 24 hpi RLs from PL and UCB relative to its own pellet. Data represent three independent experiments. The major histocompatibility complex (HLA) expression pattern is shown in RLs from PL (n = 3) and UCB (n = 2). HLA expression was observed in the center of the RLs, indicating that mesenchymal stromal cells constituted the RLs. Statistical significance was set as follows: $^{a}P < 0.05$; $^{c}P < 0.0005$. UCB: Umbilical cord blood; PL: Placenta; RL: Recombinant limb; HLA: Human leukocyte antigen.

central structure than PL-RLs. Although Alcian blue staining around the condensed cells was observed in MSCs-RLs from both sources, cell morphology analyses showed no cartilage anlage formation after 72 hpi as observed in CK-RLs (Figure 2). The lack of well-formed skeletal elements and cartilage morphology in MSCs-RLs suggests that MSCs cannot form complex skeletal structures because they can remain undifferentiated or in an early committed state. These results also suggest that PL-MSCs and UCB-MSCs respond differently to embryonic ectoderm signals.

Molecular and in situ characterization of cell differentiation in MSC-RLs

In contrast to CK-RL, histological analyses of MSCs-RLs did not indicate specific tissue formation at any evaluated time. Thus, to determine if the PL-MSCs and UCB-MSCs committed to limb cellular lineages during MSCs-RL formation, we evaluated the expression profile of chondrogenic (*Sox9, Gdf5*, *Col2a1*, *Acan,* and *Hif1a*), osteogenic (*Runx2*), and tenogenic (*Scx* and *Mkx*) differentiation genes at 24 hpi in MSCs-RLs from both sources (Figure 3A). The results confirmed that MSCs commit to limb lineages but respond differentially to embryonic ectodermal signals as the expression of molecular markers of chondrogenic, osteogenic, and tenogenic lineages was induced at different levels in MSCs-RLs from both sources compared with its initial pellet (Table 1).

Comparative analyses of *Sox9* expression levels between MSCs-RLs showed no significant differences ($P < 0.8421$), but remarkably, it was highly induced in both MSCs after receiving ectodermal signals (Figure 3A, Table 1). By contrast, low *Gdf5* expression was observed in both sources compared with its initial levels. In addition, it was significatively reduced in UCB-RLs compared with PL-RLs ($P < 0.0205$; Figure 3A, Table 1). Regarding later chondrogenic-associated genes, expression of *Col2a1* was not detected in UCB-RLs, whereas its expression was significatively reduced in PL-RLs (Figure 3A, Table 1). On the other hand, *Acan* was overexpressed only in UCB-RLs and was significatively reduced in PL-RLs ($P < 0.0001$; Figure 3A, Table 1). Interestingly, the levels of *Hif1a* observed in both MSCs-RLs suggest that a hypoxic environment is favored under these conditions (Figure 3A, Table 1). Regarding osteo-genic commitment, *Runx2* was positively regulated in both PL-RLs and UCB-RLs; however, the expression levels of this gene in UCB-RLs were significatively higher than those observed in PL-RLs ($P < 0.0001$; Figure 3A, Table 1). The tenogenic marker *Scx* was markedly induced in UCB-RLs compared with PL-RLs ($P < 0.0004$), in which expression was inhibited (Figure 3A, Table 1). By contrast, *Mkx* expression was significantly downregulated in UCB-RLs compared with PL-RLs ($P < 0.0002$; Figure 3A, Table 1). To evaluate the spatial organization of committed cells, the protein distribution of SOX9, SCX, and RUNX2 was evaluated in MSC-RLs (Figure 3B). Importantly, the high protein expression was correlated with gene expression in all RLs, as assessed by qPCR (Figure 3B, Table 1). However, these results demonstrated that the localization of SOX9, SCX, and RUNX2 was not restricted to the center of the MSCs-RLs (Figure 3B). Together, these results suggest that at 24 hpi, cells in MSCs-RLs are committed early to the chondrogenic lineage. UCB-RLs can also commit to osteogenic lineage,

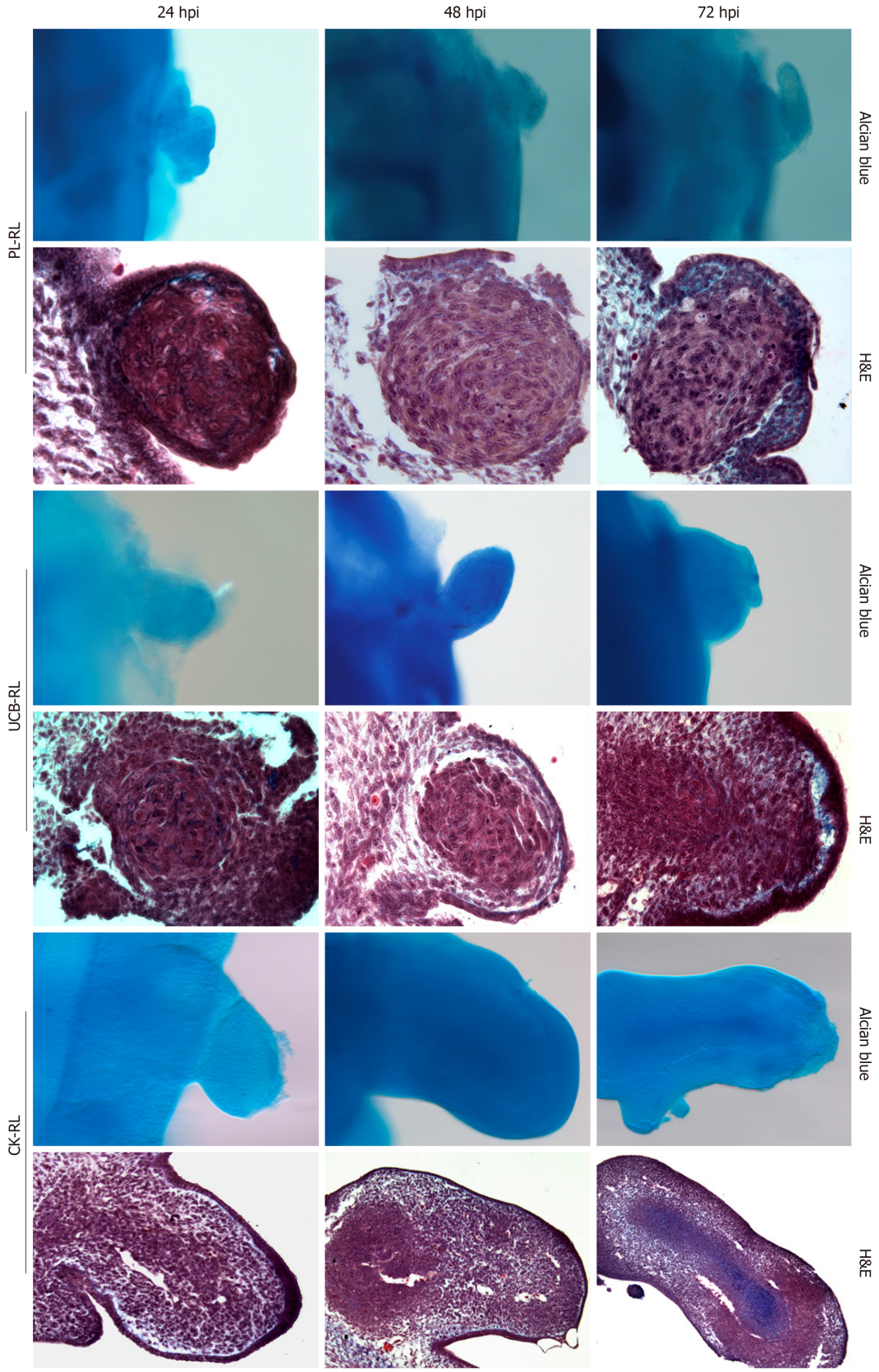

DOI: 10.4252/wjsc.v15.i7.701

Figure 2 Phenotypic and histological characterization of the mesenchymal stromal cells-recombinant limbs. Alcian blue and hematoxylin and eosin staining of recombinant limbs from the placenta (n = 8), umbilical cord blood (n = 7), and chicken (n = 4) at 24, 48, and 72 h postimplantation. hpi: Hour postimplantation; UCB: Umbilical cord blood; PL: Placenta; RL: Recombinant limb; CK: Chicken; H&E: Hematoxylin and eosin.

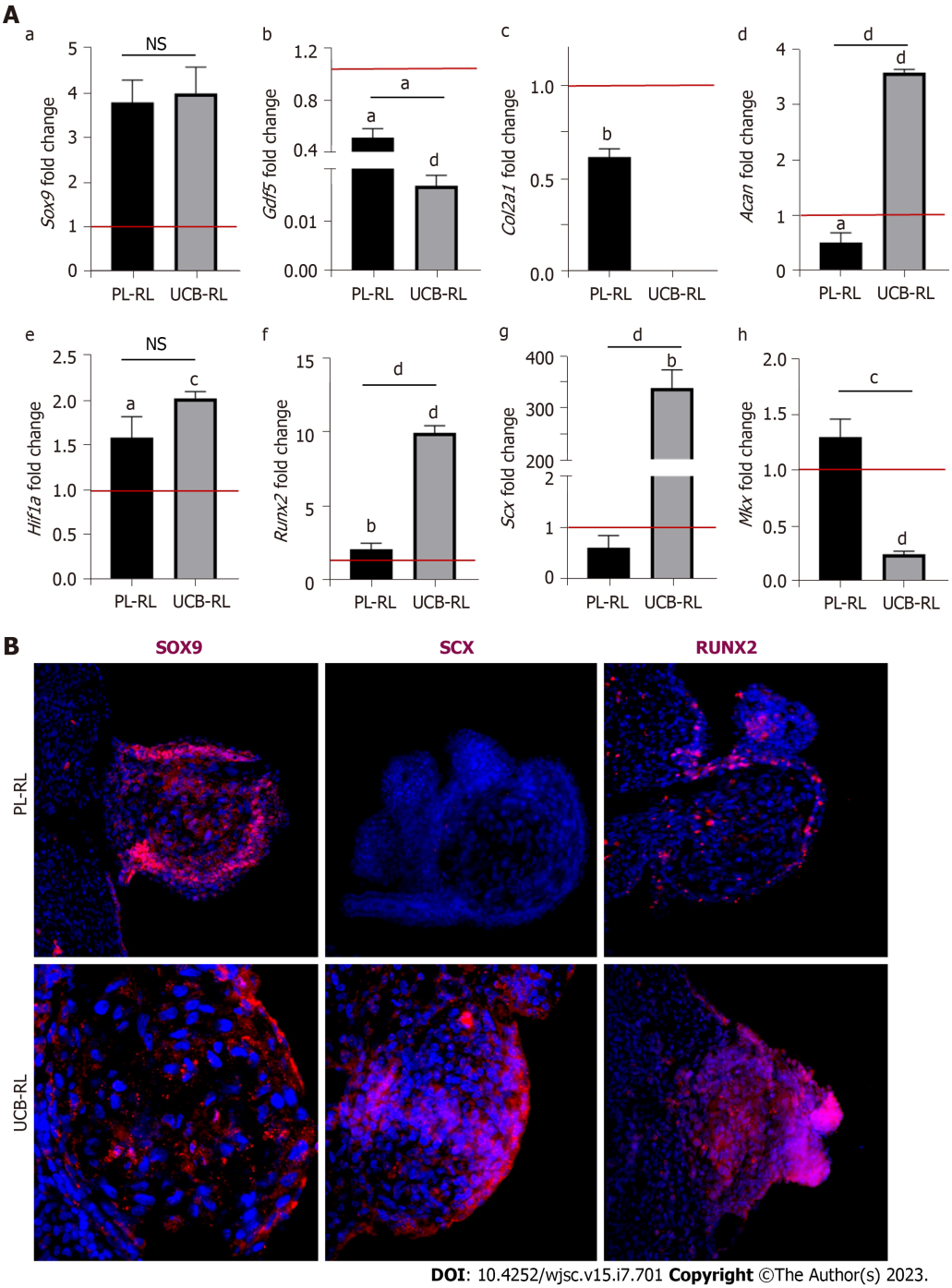

DOI: 10.4252/wjsc.v15.i7.701

Figure 3 Mesenchymal stromal cells differentially commit to chondrogenic, osteogenic, and tenogenic lineages in the recombinant limb system. A: Quantitative polymerase chain reaction analysis of cartilage (a-e), bone (f), and tendon (g and h) cell fate-regulating genes of the mesenchymal stromal cells-recombinant limbs (MSCs-RLs) at 24 h postimplantation (hpi) relative to its own pellet set to 1.0. Statistical significance comparing MSCs-RLs from the two sources is shown; B: Protein expression pattern of master genes of the three differentiation lineages in MSCs-RLs at 24 hpi. Data represent three independent experiments. Statistical significance was set as follows: $^{a}P < 0.05$; $^{b}P < 0.005$; $^{c}P < 0.0005$; $^{d}P < 0.0001$. For more details see Table 1. Sox9: SRY-box transcription factor 9; Gdf5: Growth differentiation 5; Col2α1: Collagen type 2 alpha 1; Acan: Aggecan; Hif1α: Hypoxia-inducible factor 1 alpha; Runx2: Runt-related transcription factor 2; Scx: Scleraxis; Mkx: Mohawk; UCB: Umbilical cord blood; RL: Recombinant limb; PL: Placenta; NS: Not significant.

although preferentially to a tenogenic cell fate, but this cell fate is not promoted in PL-RLs.

Evaluation of Fgf-8 expression and cell death in MSCs-RLs

Signals from the ectoderm and AER are indispensable for maintaining cell survival and proliferation during limb development and RL formation[23]. During limb development, the undifferentiated cellular state and cell commitment balance depend on signals from the AER[2]. To determine whether the lack of ectodermal signals or massive cell death was the mechanism underlying the inability of MSC to form skeletal structures, ectoderm integrity by *Fgf8* expression and lysotracker staining were evaluated in RLs (Figure 4). The results showed that the cell death process was present in

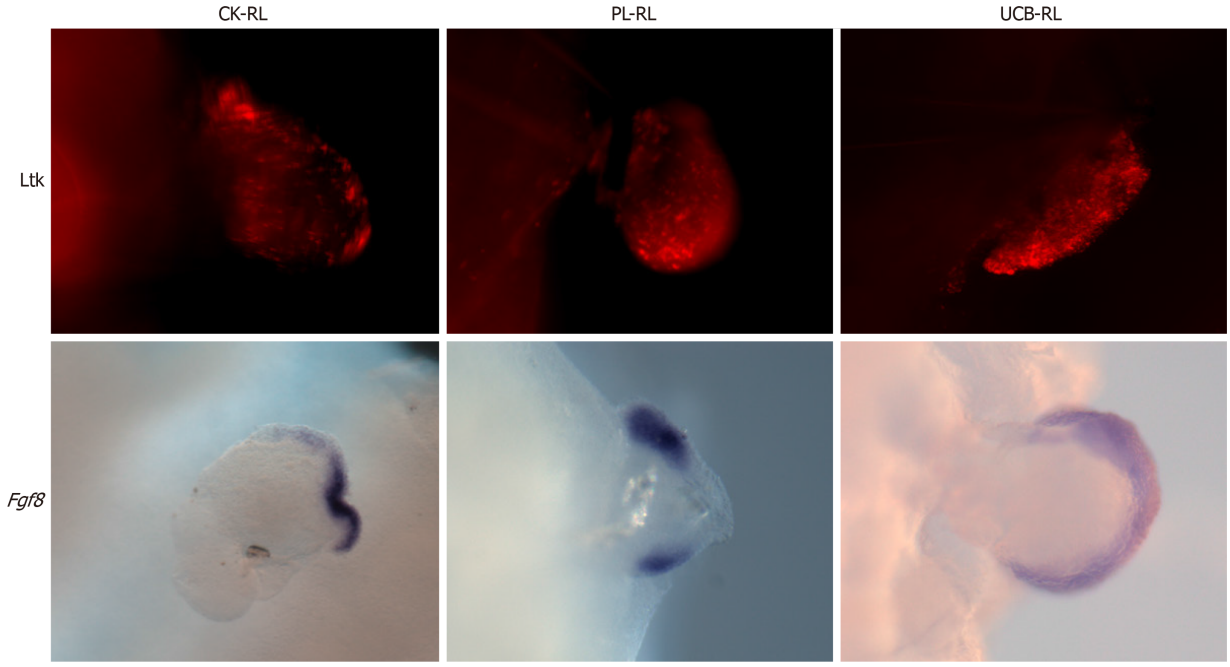

DOI: 10.4252/wjsc.v15.i7.701

Figure 4 Cell death and fibroblast growth factor 8 expression pattern in mesenchymal stromal cells and chicken recombinant limbs at 24 h postimplantation. Lysotracker staining (Ltk) to evaluate cell death in recombinant limbs (RLs) from the placenta (PL-RLs; *n* = 6), umbilical cord blood (UCB-RLs; *n* = 6), and chicken (CK-RLs; *n* = 4) is shown. *In situ* hybridization of fibroblast growth factor 8 (*Fgf8*) in PL-RLs showed disrupted pattern of this gene in 2/4 RLs; *Fgf8* expression in UCB-RLs was detected in 3/6 evaluated samples, while 5/5 CK-RLs continued to express *Fgf-8* at 24 h postimplantation. UCB: Umbilical cord blood; PL: Placenta; RL: Recombinant limb; CK: Chicken; Ltk: Lysotracker staining; Fgf8: Fibroblast growth factor 8.

the ectoderm of all evaluated RLs; UCB-RLs showed a higher number of dead cells than PL-RLs and CK-RLs. Interestingly, in PL-RLs and CK-RLs, dead cells were concentrated in the apical area of the ectoderm, whereas in UCB-RLs, dead cells were distributed homogeneously on the ectoderm of all samples evaluated (Figure 4). Despite the death of ectodermal cells, *Fgf8* expression was maintained in some MSCs-RLs (see details in the figure legend) or its expression in PL-RLs was disrupted in the center of the ectoderm (Figure 4). These results suggest that at 24 hpi, signals continue to emanate from the AER, which are received by the MSCs or CK-LBMCs beneath the AER.

DISCUSSION

Cells commit to specific lineages once the expression of master genes occurs in response to inducing factors. However, the ability to interpret signals and acquire a particular fate and behavior depend on the developmental history of the cells. The capacity to organize complex structures depends on cell differentiation, cell recruitment, cell movement, differential cell proliferation, and cell death, which occur during the morphogenetic process of tissues and organs.

In this study, we used the RL model to evaluate the morphogenetic abilities of MSCs other than those observed in cell culture. Because RLs provide limb spatial-temporal signals, we evaluated the ability of MSCs to generate complex skeletal structures[23-25]. We found that human MSCs can integrate into an RL implanted in the CK embryo. PL- or UCB-MSCs from RLs respond differently to ectodermal signals, suggesting that the source of MSCs might be important to delineate a particular lineage *in vivo* (Figure 5). Although MSCs from both sources start the chondrogenic program with high levels of SOX9 expression, they do not necessarily equally follow and complete the cell differentiation process (Figure 5). *In vitro* studies have shown that UCB-MSCs preferentially differentiate into osteogenic lineages[17] and present a higher *in vivo* osteogenic and chondrogenic differentiation potential than BM-MSCs when grafted subcutaneously with a scaffold of hydroxyapatite/tricalcium phosphate[19]. By contrast, PL-MSCs preferentially differentiate into an osteogenic lineage when seeded into microcarriers or nanofiber scaffolds[20,21]. These findings suggest that depending on the tissue source, MSCs can represent a cell population with a different number of osteogenic or chondrogenic progenitors or both. Similarly, the molecular markers from chondrogenic and osteogenic lineages were induced at higher levels in UCB-RLs than in PL-RLs. However, the high expression levels of *Runx2* and *Scx* genes did not lead to the formation of well-defined bone tissue or tendons. In addition, the gene expression pattern of *Sox9, Scx,* and *Rux2* did not associate with a specific tissue pattern or arrangement inside the RLs. The expression of molecular markers was not sufficient to promote the formation of well-defined structures, likely because the morphogenetic program was not triggered. Interestingly, PL-RLs expressed high levels of *Mkx* while UCB-RL expressed high levels of *Scx*. It is unknown if in this system both genes are needed to form well-structured tendons. Nevertheless, the expression of *Mkx* or *Scx* can drive the *in vitro* differentiation of BM-MSCs to a tenocyte fate[13,27].

Table 1 Analysis of gene expression fold-changes of differentiation genes between pellets and their corresponding recombinant limbs of different mesenchymal stromal cell sources at 24 h postimplantation

Source	*Sox9*	*Col2a1*	*Acan*	*Gdf5*	*Hif1α*	*Runx2*	*Scx*	*Mkx*
UCB-RL *vs* UCB-pellet	3.99 ± 0.4, $P <$ 0.0004	ND	3.58 ± 0.10, $P <$ 0.0001	0.01 ± 00.003, $P <$ 0.0001	1.58 ± 0.79, $P <$ 0.0002	9.96 ± 0.65 $P <$ 0.0001	377.61 ± 78.24, $P <$ 0.002	0.24 ± 0.03, $P <$ 0.0001
PL-RL *vs* PL-pellet	3.79 ± 0.4, $P <$ 0.0007	0.61 ± 0.12, $P <$ 0.002	0.55 ± 0.21, $P <$ 0.052	0.56 ± 0.12, $P <$ 0.01	1.61 ± 0.28, $P <$ 0.03	2.18 ± 0.59, $P <$ 0.03	0.61 ± 0.33, $P <$ 0.14	1.29 ± 0.22, $P <$ 0.21

Gene expression fold-change was evaluated comparing the pellet of mesenchymal stromal cells (MSCs) after forming the recombinant limb (RL) with MSCs-RLs from both sources. Data from the pellet were set to 1.0. Statistical significance comparing placenta-RL *vs* umbilical cord blood-RL is shown in Figure 3A. All data are presented as mean ± SD. Statistical significance was set at $P < 0.05$. Acan: Aggecan; Col2α1: Collagen type 2 alpha 1; Gdf5: Growth differentiation 5; Hif1α: Hypoxia-inducible factor 1 alpha; Mkx: Mohawk; ND: Not detected; Scx: Scleraxis; Sox9: SRY-box transcription factor 9; Runx2: Runt-related transcription factor 2; UCB: Umbilical cord blood; RL: Recombinant limb; PL: Placenta.

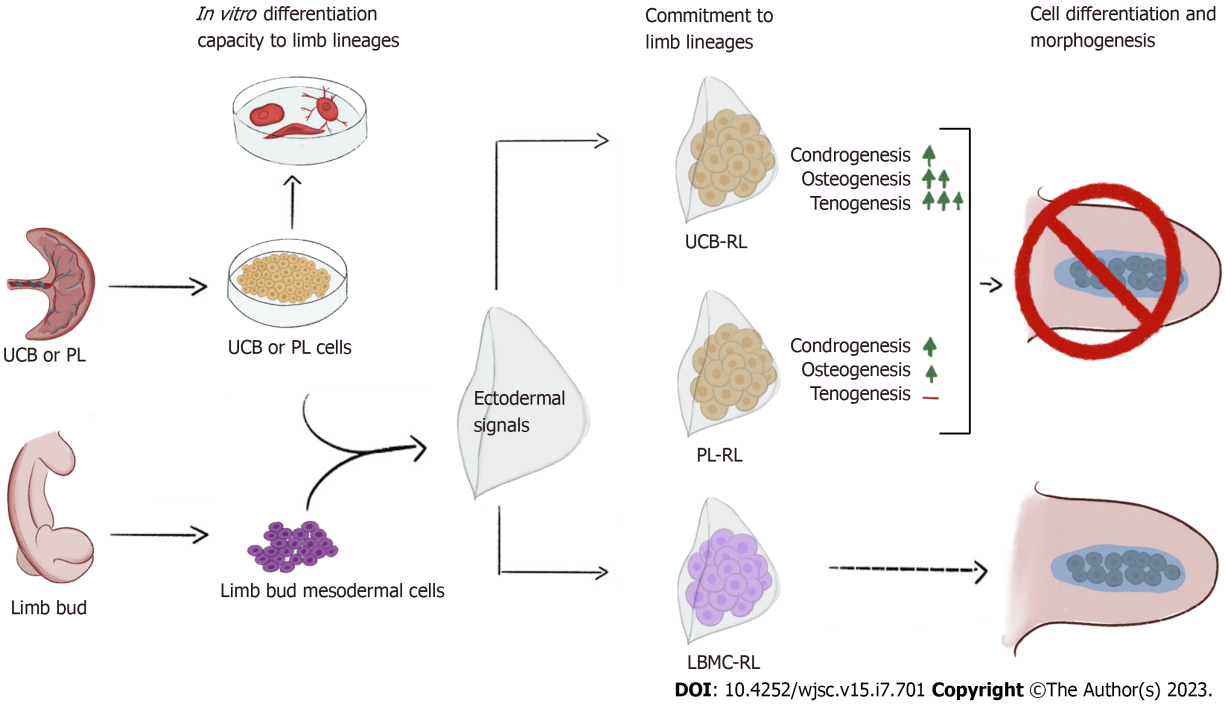

DOI: 10.4252/wjsc.v15.i7.701

Figure 5 Mesenchymal stromal cells commit to limb mesodermal lineages but are not capable of forming skeletal structures. Mesenchymal stromal cells (MSCs) from umbilical cord blood (UCB) and placenta (PL) differentiated into chondrogenic, osteogenic, and tenogenic lineages *in vitro*. However, under the influence of differentiation and morphogenetic signals from limb ectoderm in the recombinant limb (RL) system, MSCs committed to limb lineages but failed to organize into tridimensional structures and form skeletal elements as observed with limb bud mesodermal cells under the same conditions. Similarly, the response to ectodermal signals depended on the source of MSCs: UCB-RLs had higher expression of osteogenic and tenogenic markers than PL-RLs, whereas in PL-RLs, tenogenic markers were downregulated after receiving ectodermal signals. UCB: Umbilical cord blood; PL: Placenta; LBMC: Limb bud mesodermal cell; RL: Recombinant limb.

The inability of MSCs to generate complex structures suggests that MSC populations, in addition to being composed of a wide variety of cell types, are unable to initiate or follow a morphogenetic program *in vivo*. Although MSCs can differentiate into skeletal lineages, it does not guarantee that they will organize into skeletal elements. It is possible that the RL model lacks signals to support the formation of skeletal elements. However, CK-LBMCs respond to differentiation signals, resulting in the generation of skeletal elements. Thus, the RL system provides signals that instruct cells to form skeletal elements.

We did not observe exacerbated cell death in the MSCs-RLs, but in some MSCs-RLs the loss of *Fgf8* expression in the AER was evident. Additional studies are needed to determine if this cell death results from the loss of FGF8 loop signaling between the AER and MSCs, or if MSCs cannot recover and maintain the loop to maintain FGF8 expression. Our data suggest that the differentiation process in MSCs is detached from the process of morphogenesis and patterning, although it is possible that addi-tional signals may be needed to promote the integration of morphogenetics with differentiation signals in MSCs. Accordingly, other studies have shown that after implantation in the kidney subcapsular region or nude mice[28-31], MSCs organize better than *in vitro* but never originate complex structures such as skeletal elements or other limb musculoskeletal tissues.

Although MSCs are considered relevant in regenerative medicine, their intrinsic cellular properties may explain why the reported therapeutic effects of MSCs are mostly indirect through immunomodulation or paracrine mechanisms rather than reliable integration into adult tissues or *de novo* tissue forma-tion[32-39].

CONCLUSION

This study demonstrates that the expression of differentiation markers of skeletal lineages in MSCs is not sufficient to generate skeletal structures *in vivo*, possibly due to the intrinsic characteristics of MSCs. In regenerative medicine, cells must be incorporated into well-defined tissues or generate new complex structures with a well-defined patterning. Thus, further application of MSCs in regenerative medicine needs to focus on understanding their biological characteristics to gain insights into how MSCs can integrate into adult tissues or properly rebuild tissues and organs.

ARTICLE HIGHLIGHTS

Research background

Mesenchymal stem cells (MSCs) differentiate *in vitro* to different skeletal lineages; however, it is un-known if they have the ability to form complex skeletal structures.

Research motivation

Although MSCs are considered relevant in regenerative medicine, reliable integration into adult tissues or *de novo* tissue formation has not been demonstrated. The application of MSCs in regenerative medicine needs to focus on understanding their biological characteristics to gain insights into how MSCs can integrate into adult tissues or properly rebuild tissues and organs.

Research objectives

To evaluate the ability of MSCs to organize and form complex skeletal structures *in vivo* under the influ-ence of embryonic signals.

Research methods

The recombinant limb (RL) is an experimental system that recapitulates the embryonic environment and its influence on cells to generate skeletal structures. Here, umbilical cord blood (UCB)-MSCs or placenta (PL)-MSCs were placed in an RL to assess their ability to form skeletal structures. The evaluation was conducted by Alcian blue staining, immunofluor-escence, and quantitative polymerase chain reaction of molecular markers of skeletal lineages.

Research results

MSCs expressed molecular markers of skeletal lineages but were unable to generate complex skeletal structures. PL-MSCs or UCB-MSCs integrated into an RL implanted in a chicken embryo. They res-ponded differently to ectodermal signals starting the chondrogenic, osteogenic, or tenogenic program with high *SRY-box transcription factor 9*, *Runt-related transcription factor 2*, and *scleraxis* gene expression levels. However, PL-MSCs or UCB-MSCs did not complete the cell differentiation and morphogenetic processes, likely due to the intrinsic characteristics of MSCs.

Research conclusions

PL-MSCs or UCB-MSCs express molecular markers of skeletal lineages but do not organize into com-plex skeletal structures. The use of RLs is an excellent model for determining the ability of cells from other origins than limb bud mesodermal cells to generate skeletal structures. The inability of MSCs to form skeletal structures might be due to their intrinsic characteristics. Additional studies are needed to understand the properties of MSCs and whether they can integrate into adult tissues or properly rebuild tissues and organs.

Research perspectives

The application of MSCs to regenerative medicine needs to focus on understanding their biological characteristics to gain insights into how MSCs can integrate into adult tissues or properly rebuild tissues and organs.

ACKNOWLEDGEMENTS

The authors thank Maria Valeria Chimal-Montes de Oca for her artwork.

FOOTNOTES

Author contributions: Marín-Llera JC and Chimal-Monroy J conceptualized the research and wrote the manuscript; Marín-Llera JC, Montesinos-Montesinos JJ, and Chimal-Monroy J discussed the data; Marín-Llera JC, García-García RD, and Garay-Pacheco E performed the experiments; Adrian Cortes-Morales V maintained and prepared the mesenchymal stromal cells; and all authors approved the final version of the manuscript.

Supported by the Dirección General de Asuntos del Personal Académico (DGAPA)-Universidad Nacional Autónoma de México, No. IN211117; Consejo Nacional de Ciencia y Tecnología (CONACyT), No. 1887 CONACyT-Fronteras de la Ciencia awarded to Chimal-Monroy J; García-García RD and Garay-Pacheco E received an undergraduate scholarship; and Marin-Llera JC a postdoctoral fellowship from the Consejo Nacional de Ciencia y Tecnología, No. CONACyT-Fronteras de la Ciencia-1887.

Institutional review board statement: The studies involving human cells were reviewed and approved by the Institutional Review Board for health research of the Instituto Mexicano del Seguro Social (IMSS, Mexico City, Mexico).

Institutional animal care and use committee statement: The handling protocol for the use of chicken embryos was done in embryonic stages in which the embryos do not feel pain because the nervous system development is not yet complete.

Conflict-of-interest statement: All the authors report no relevant conflicts of interest for this article.

Data sharing statement: No additional data are available.

ARRIVE guidelines statement: The authors have read the ARRIVE guidelines, and the manuscript was prepared and revised according to the ARRIVE guidelines.

Country/Territory of origin: Mexico

ORCID number: Jessica Cristina Marín-Llera 0000-0002-1221-5258; Juan Jose Montesinos-Montesinos 0000-0002-1042-3205; Jesus Chimal-Monroy 0000-0002-6511-7408.

S-Editor: Wang JJ
L-Editor: A
P-Editor: Wang JJ

REFERENCES

1 **Zeller R**, López-Ríos J, Zuniga A. Vertebrate limb bud development: moving towards integrative analysis of organogenesis. *Nat Rev Genet* 2009; **10**: 845-858 [PMID: 19920852 DOI: 10.1038/nrg2681]
2 **Marín-Llera JC**, Garciadiego-Cázares D, Chimal-Monroy J. Understanding the Cellular and Molecular Mechanisms That Control Early Cell Fate Decisions During Appendicular Skeletogenesis. *Front Genet* 2019; **10**: 977 [PMID: 31681419 DOI: 10.3389/fgene.2019.00977]
3 **Chimal-Monroy J**, Rodriguez-Leon J, Montero JA, Gañan Y, Macias D, Merino R, Hurle JM. Analysis of the molecular cascade responsible for mesodermal limb chondrogenesis: Sox genes and BMP signaling. *Dev Biol* 2003; **257**: 292-301 [PMID: 12729559 DOI: 10.1016/s0012-1606(03)00066-6]
4 **Lefebvre V**, Behringer RR, de Crombrugghe B. L-Sox5, Sox6 and Sox9 control essential steps of the chondrocyte differentiation pathway. *Osteoarthritis Cartilage* 2001; **9** Suppl A: S69-S75 [PMID: 11680692 DOI: 10.1053/joca.2001.0447]
5 **Buxton P**, Edwards C, Archer CW, Francis-West P. Growth/differentiation factor-5 (GDF-5) and skeletal development. *J Bone Joint Surg Am* 2001; **83-A** Suppl 1: S23-S30 [PMID: 11263662 DOI: 10.1016/j.jclinepi.2014.04.006]
6 **Merino R**, Macias D, Gañan Y, Economides AN, Wang X, Wu Q, Stahl N, Sampath KT, Varona P, Hurle JM. Expression and function of Gdf-5 during digit skeletogenesis in the embryonic chick leg bud. *Dev Biol* 1999; **206**: 33-45 [PMID: 9918693 DOI: 10.1006/dbio.1998.9129]
7 **Amarilio R**, Viukov SV, Sharir A, Eshkar-Oren I, Johnson RS, Zelzer E. HIF1alpha regulation of Sox9 is necessary to maintain differentiation of hypoxic prechondrogenic cells during early skeletogenesis. *Development* 2007; **134**: 3917-3928 [PMID: 17913788 DOI: 10.1242/dev.008441]
8 **Chen H**, Ghori-Javed FY, Rashid H, Adhami MD, Serra R, Gutierrez SE, Javed A. Runx2 regulates endochondral ossification through control of chondrocyte proliferation and differentiation. *J Bone Miner Res* 2014; **29**: 2653-2665 [PMID: 24862038 DOI: 10.1002/jbmr.2287]
9 **Otto F**, Thornell AP, Crompton T, Denzel A, Gilmour KC, Rosewell IR, Stamp GW, Beddington RS, Mundlos S, Olsen BR, Selby PB, Owen MJ. Cbfa1, a candidate gene for cleidocranial dysplasia syndrome, is essential for osteoblast differentiation and bone development. *Cell* 1997; **89**: 765-771 [PMID: 9182764 DOI: 10.1016/s0092-8674(00)80259-7]
10 **Komori T**, Yagi H, Nomura S, Yamaguchi A, Sasaki K, Deguchi K, Shimizu Y, Bronson RT, Gao YH, Inada M, Sato M, Okamoto R, Kitamura Y, Yoshiki S, Kishimoto T. Targeted disruption of Cbfa1 results in a complete lack of bone formation owing to maturational arrest of osteoblasts. *Cell* 1997; **89**: 755-764 [PMID: 9182763 DOI: 10.1016/s0092-8674(00)80258-5]
11 **Schweitzer R**, Chyung JH, Murtaugh LC, Brent AE, Rosen V, Olson EN, Lassar A, Tabin CJ. Analysis of the tendon cell fate using Scleraxis,

a specific marker for tendons and ligaments. *Development* 2001; **128**: 3855-3866 [PMID: 11585810 DOI: 10.1242/dev.128.19.3855]

12 **Murchison ND**, Price BA, Conner DA, Keene DR, Olson EN, Tabin CJ, Schweitzer R. Regulation of tendon differentiation by scleraxis distinguishes force-transmitting tendons from muscle-anchoring tendons. *Development* 2007; **134**: 2697-2708 [PMID: 17567668 DOI: 10.1242/dev.001933]

13 **Ito Y**, Toriuchi N, Yoshitaka T, Ueno-Kudoh H, Sato T, Yokoyama S, Nishida K, Akimoto T, Takahashi M, Miyaki S, Asahara H. The Mohawk homeobox gene is a critical regulator of tendon differentiation. *Proc Natl Acad Sci U S A* 2010; **107**: 10538-10542 [PMID: 20498044 DOI: 10.1073/pnas.1000525107]

14 **Lejard V**, Blais F, Guerquin MJ, Bonnet A, Bonnin MA, Havis E, Malbouyres M, Bidaud CB, Maro G, Gilardi-Hebenstreit P, Rossert J, Ruggiero F, Duprez D. EGR1 and EGR2 involvement in vertebrate tendon differentiation. *J Biol Chem* 2011; **286**: 5855-5867 [PMID: 21173153 DOI: 10.1074/jbc.M110.153106]

15 **Huang Y**, Wu Q, Tam PKH. Immunomodulatory Mechanisms of Mesenchymal Stem Cells and Their Potential Clinical Applications. *Int J Mol Sci* 2022; **23** [PMID: 36077421 DOI: 10.3390/ijms231710023]

16 **Aguiar Koga BA**, Fernandes LA, Fratini P, Sogayar MC, Carreira ACO. Role of MSC-derived small extracellular vesicles in tissue repair and regeneration. *Front Cell Dev Biol* 2022; **10**: 1047094 [PMID: 36935901 DOI: 10.3389/fcell.2022.1047094]

17 **Lee RH**, Kim B, Choi I, Kim H, Choi HS, Suh K, Bae YC, Jung JS. Characterization and expression analysis of mesenchymal stem cells from human bone marrow and adipose tissue. *Cell Physiol Biochem* 2004; **14**: 311-324 [PMID: 15319535 DOI: 10.1159/000080341]

18 **Sacchetti B**, Funari A, Remoli C, Giannicola G, Kogler G, Liedtke S, Cossu G, Serafini M, Sampaolesi M, Tagliafico E, Tenedini E, Saggio I, Robey PG, Riminucci M, Bianco P. No Identical "Mesenchymal Stem Cells" at Different Times and Sites: Human Committed Progenitors of Distinct Origin and Differentiation Potential Are Incorporated as Adventitial Cells in Microvessels. *Stem Cell Reports* 2016; **6**: 897-913 [PMID: 27304917 DOI: 10.1016/j.stemcr.2016.05.011]

19 **Igura K**, Zhang X, Takahashi K, Mitsuru A, Yamaguchi S, Takashi TA. Isolation and characterization of mesenchymal progenitor cells from chorionic villi of human placenta. *Cytotherapy* 2004; **6**: 543-553 [PMID: 15770794 DOI: 10.1080/14653240410005366-1]

20 **Zhang D**, Tong A, Zhou L, Fang F, Guo G. Osteogenic differentiation of human placenta-derived mesenchymal stem cells (PMSCs) on electrospun nanofiber meshes. *Cytotechnology* 2012; **64**: 701-710 [PMID: 22526490 DOI: 10.1007/s10616-012-9450-5]

21 **García-García RD**, Garay-Pacheco E, Marín-Llera JC, Chimal-Monroy J. Recombinant Limb Assay as in Vivo Organoid Model. *Front Cell Dev Biol* 2022; **10**: 863140 [PMID: 35557939 DOI: 10.3389/fcell.2022.863140]

22 **Elisa Piedra M**, Borja Rivero1 F, Fernandez-Teran M, Ros MA. Pattern formation and regulation of gene expressions in chick recombinant limbs. *Mech Dev* 2000; **90**: 167-179 [PMID: 10640702 DOI: 10.1016/s0925-4773(99)00247-6]

23 **Ros MA**, Lyons GE, Mackem S, Fallon JF. Recombinant limbs as a model to study homeobox gene regulation during limb development. *Dev Biol* 1994; **166**: 59-72 [PMID: 7958460 DOI: 10.1006/dbio.1994.1296]

24 **Marín-Llera JC**, Fernández-Calderón M, Chimal-Monroy J. Chicken Recombinant Limbs Assay to Understand Morphogenesis, Patterning, and Early Steps in Cell Differentiation. *J Vis Exp* 2022; **2022**: 179 [PMID: 35098947 DOI: 10.3791/63183]

25 **Montesinos JJ**, Flores-Figueroa E, Castillo-Medina S, Flores-Guzmán P, Hernández-Estévez E, Fajardo-Orduña G, Orozco S, Mayani H. Human mesenchymal stromal cells from adult and neonatal sources: comparative analysis of their morphology, immunophenotype, differentiation patterns and neural protein expression. *Cytotherapy* 2009; **11**: 163-176 [PMID: 19152152 DOI: 10.1080/14653240802582075]

26 **Hamburger V**, Hamilton HL. A series of normal stages in the development of the chick embryo. 1951. *Dev Dyn* 1992; **195**: 231-272 [PMID: 1304821 DOI: 10.1002/aja.1001950404]

27 **Liu H**, Zhang C, Zhu S, Lu P, Zhu T, Gong X, Zhang Z, Hu J, Yin Z, Heng BC, Chen X, Ouyang HW. Mohawk promotes the tenogenesis of mesenchymal stem cells through activation of the TGFβ signaling pathway. *Stem Cells* 2015; **33**: 443-455 [PMID: 25332192 DOI: 10.1002/stem.1866]

28 **Almeida A**, Lira R, Oliveira M, Martins M, Azevedo Y, Silva KR, Carvalho S, Cortez E, Stumbo AC, Carvalho L, Thole A. Bone marrow-derived mesenchymal stem cells transplantation ameliorates renal injury through anti-fibrotic and anti-inflammatory effects in chronic experimental renovascular disease. *Biomed J* 2022; **45**: 629-641 [PMID: 34333108 DOI: 10.1016/j.bj.2021.07.009]

29 **Rackham CL**, Chagastelles PC, Nardi NB, Hauge-Evans AC, Jones PM, King AJ. Co-transplantation of mesenchymal stem cells maintains islet organisation and morphology in mice. *Diabetologia* 2011; **54**: 1127-1135 [PMID: 21267536 DOI: 10.1007/s00125-011-2053-4]

30 **Fu Z**, Chu Y, Geng X, Ma Y, Chi K, Song C, Liao S, Hong Q, Wu D, Wang Y. Artificial Kidney Capsule Packed with Mesenchymal Stem Cell-Laden Hydrogel for the Treatment of Rhabdomyolysis-Induced Acute Kidney Injury. *ACS Biomater Sci Eng* 2022; **8**: 1726-1734 [PMID: 35302761 DOI: 10.1021/acsbiomaterials.1c01595]

31 **Kumar S**, Wan C, Ramaswamy G, Clemens TL, Ponnazhagan S. Mesenchymal stem cells expressing osteogenic and angiogenic factors synergistically enhance bone formation in a mouse model of segmental bone defect. *Mol Ther* 2010; **18**: 1026-1034 [PMID: 20068549 DOI: 10.1038/mt.2009.315]

32 **Gao F**, Chiu SM, Motan DA, Zhang Z, Chen L, Ji HL, Tse HF, Fu QL, Lian Q. Mesenchymal stem cells and immunomodulation: current status and future prospects. *Cell Death Dis* 2016; **7**: e2062 [PMID: 26794657 DOI: 10.1038/cddis.2015.327]

33 **Sarsenova M**, Kim Y, Raziyeva K, Kazybay B, Ogay V, Saparov A. Recent advances to enhance the immunomodulatory potential of mesenchymal stem cells. *Front Immunol* 2022; **13**: 1010399 [PMID: 36211399 DOI: 10.3389/fimmu.2022.1010399]

34 **Wang M**, Yuan Q, Xie L. Mesenchymal Stem Cell-Based Immunomodulation: Properties and Clinical Application. *Stem Cells Int* 2018; **2018**: 3057624 [PMID: 30013600 DOI: 10.1155/2018/3057624]

35 **Xiang XN**, Zhu SY, He HC, Yu X, Xu Y, He CQ. Mesenchymal stromal cell-based therapy for cartilage regeneration in knee osteoarthritis. *Stem Cell Res Ther* 2022; **13**: 14 [PMID: 35012666 DOI: 10.1186/s13287-021-02689-9]

36 **Waterman RS**, Tomchuck SL, Henkle SL, Betancourt AM. A new mesenchymal stem cell (MSC) paradigm: polarization into a pro-inflammatory MSC1 or an Immunosuppressive MSC2 phenotype. *PLoS One* 2010; **5**: e10088 [PMID: 20436665 DOI: 10.1371/journal.pone.0010088]

37 **Tomchuck SL**, Zwezdaryk KJ, Coffelt SB, Waterman RS, Danka ES, Scandurro AB. Toll-like receptors on human mesenchymal stem cells drive their migration and immunomodulating responses. *Stem Cells* 2008; **26**: 99-107 [PMID: 17916800 DOI: 10.1634/stemcells.2007-0563]

38 **Fu Y**, Karbaat L, Wu L, Leijten J, Both SK, Karperien M. Trophic Effects of Mesenchymal Stem Cells in Tissue Regeneration. *Tissue Eng Part B Rev* 2017; **23**: 515-528 [PMID: 28490258 DOI: 10.1089/ten.TEB.2016.0365]

39 **Hofer HR**, Tuan RS. Secreted trophic factors of mesenchymal stem cells support neurovascular and musculoskeletal therapies. *Stem Cell Res Ther* 2016; **7**: 131 [PMID: 27612948 DOI: 10.1186/s13287-016-0394-0]

Published by **Baishideng Publishing Group Inc**
7041 Koll Center Parkway, Suite 160, Pleasanton, CA 94566, USA
Telephone: +1-925-3991568
E-mail: bpgoffice@wjgnet.com
Help Desk: https://www.f6publishing.com/helpdesk
https://www.wjgnet.com